Desalination and Water Treatment
www.deswater.com
doi: 10.5004/dwt.2017.20979

87 (2017) 188–198
August

Use of natural Tunisian clays for defluoridation of industrial wastewater

Abdessalem Ezzeddine*, Ahmed Hannachi

Department of Chemical-Process Engineering, National School of Engineering of Gabes, University of Gabes, Omar Ibn Elkhattab Street 6072 Zrig, Gabes, Tunisia, Tel. +21698438437, Fax +21675297200, email: abdessalem.ezzeddine@enig.rnu.tn (A. Ezzeddine), ahmed.hannachi@enig.rnu.tn (A. Hannachi)

Received 1 August 2016; Accepted 25 May 2017

ABSTRACT

The aluminum fluoride manufacturing generates large amounts of wastewaters containing fluoride (AFMW). The aim of this study was to investigate the removal of fluoride from AFMW using natural Tunisian clay as an adsorbent. X-ray fluorescence analysis showed that SiO_2 (30.7%) and CaO (26.3%) were the major constituents of clay. Batch experiments were performed to study the influence of initial fluoride concentration (525–2003 mg/L), adsorbent dose (0.5–5 g/L) and initial pH (2 to 11). Kinetic tests showed that fluoride sorption to natural clay reached equilibrium after around 2 h. An optimal value of pH 2 was observed. The experimental data showed the data could be fit to Langmuir and Freundlich isotherm. Pseudo-second-order rate and an intra-particle kinetic model fit well the adsorption kinetic data. It was found that intraparticle diffusion contributes to the rate of removal of fluoride. Fourier transform infrared analysis and X-ray diffraction patterns of the adsorbent before and after adsorption indicated that fluoride ions were chemisorbed by this adsorbent. Results from this study demonstrated potential use of Tunisian clay in defluoridation of AFMW.

Keywords: Natural clay; Aluminum fluoride manufacturing; Batch experiment; Defluoridation; Adsorption; Isotherms

---

1. Introduction

Water supply sources may contain a wide variety of physical and chemical components that pose a threat to public health such as fluoride. According to several studies, long-term ingestion of water that contains fluoride can cause a reduction of protein synthesis and functional damages in such organs as thyroid, kidney, and liver [1,2]. As a result, the US EPA has set a concentration of 1.5 mg/L as the maximum allowable fluoride concentration level for drinking water. The same standards are adopted in Tunisia. However, the fluoride content usually exceeds the acceptable standards in many regions of southern Tunisia. Fluoride contamination in this region is attributed essentially to local industry including about 80% of Tunisian plants of phosphoric acid and mineral fertilizers manufacturing and a factory of aluminium fluoride production. Hence, large quantities of wastewaters containing fluoride are released from these processes and discharged in the environment. For instance the fluoride concentrations of 131–2000 mg/L and pH ~2 are found in typical wastewater from aluminum fluoride manufacturer. Effective treatment of wastewater containing fluoride is therefore a major concern in Tunisia to meet the regulatory and environmental requirements increasingly more complex, strict and evolutionary. The current discharge standards for wastewater containing fluoride vary from country to country. For instance, the recommended values for some countries are reflected in Table 1.

Examination of Table 1 shows that Tunisia is among the most stringent countries with respect to fluoride contents.

When the fluoride concentration is high, lime treatment is commonly used to precipitate fluorite (CaF_2). Although the theoretical solubility of CaF_2 is 17 mg/L at 25°C in water [9], CaF_2 precipitation can only reduce the fluoride concentration to 10–20 mg/L in practice. Depending on

---

*Corresponding author.

Presented at the EDS conference on Desalination for the Environment: Clean Water and Energy, Rome, Italy, 22-26 May 2016

1944-3994 / 1944-3986

Table 1
Discharge standards of fluoride in wastewater

Country	Norms (mg/L)	Reference
USA	4	[3]
Tunisia	3–5	[4]
Japan	5–15	[5]
China	10	[6]
France	15	[7]
Poland	25	[8]

the discharge standards for industrial wastewater shown in Table 1, a subsequent step may be necessary. Adsorption is commonly used mainly because of cost-effectiveness and simplicity of operation [10–32]. In this step, the water containing 10–20 mg/L fluoride is usually passed through different adsorbents, such as limestone, double layered hydroxides, activated alumina, aluminum alginate particles, aluminum and doping chitosan-Fe(III) hydrogel, composite materials like Ca-Al-La, biomaterial loaded with metal ion such as carboxymethyl cellulose loaded with zirconium, synthesized materials for example CaO loaded mesoporous Al_2O_3, hydrous ferric oxide, etc [33–39].

Availability of clay in nature and its high potential toward the adsorption of organic and inorganic compounds have attracted the attention of many researchers to use it for the removal of fluoride [40]. They have examined the adsorption of fluoride to china clay [41], fluoride removal by montmorillonite under various contact times and temperatures [42], treatment of high fluoride solution by Mg/Al layered double hydroxide [43], and fluoride adsorption to montmorillonite with and without calcium [44]. They also investigated the removal of fluoride by acid activated kaolinite [45], adsorption of fluoride to metal oxide incorporated bentonite [46], enhancement of fluoride removal by chemically modified bentonite with magnesium chloride [47], and fluoride ion removal by organosmectites [48].

In Tunisia, clays are abundant substances and are among the valuable materials whose valorization is important to the economy. Recently, clays and clay minerals have been examined as adsorbents for the removal of contaminants such as heavy metals [49–53], viruses, pesticides, herbicides, toluene, and other toxins [54], and smectite from northeast of Tunisia has been used for fluoride removal from aqueous solution [48]. Further experiments will improve our knowledge regarding the potential uptake of fluoride by clayey soils from southern Tunisia.

With the current shortage of water in Tunisia and the increased demands on fresh water, it is important to treat wastewater collected from aluminium fluoride industry. Therefore, this paper discusses a method using clayey soils from southern Tunisia as an adsorbent for the removal of fluoride. The characteristics of the clay were elucidated using X-ray fluorescence (XRF), X-ray diffraction (XRD) and Fourier transform infrared (FTIR) spectrometers. Equilibrium and kinetic studies were performed to examine the adsorption of fluoride by clay. Finally, the effects of adsorbent amount, pH, and initial fluoride concentration were instigated.

2. Materials and methods

2.1. Chemicals and reagents

All chemicals used in the present study were of analytical reagent grade. Sodium hydroxide (NaOH), sodium fluoride (NaF), silver chloride (AgCl) and sodium chloride (NaCl), were purchased from Scharlau Chemie S.A. (Spain). Double distilled water was used in all the experimental runs.

2.2. Purification of the clay

The clay used in this study was collected from the deposit of ″Djebel Estah″ (DE), located in southern Tunisia not far from the plant of production of aluminum fluoride. Before being used as adsorbent, the clay has undergone purification steps to remove some impurities and homogenize the grain size. This was achieved by dispersing the crude lumps in deionised water (1 kg/10 L). The mixture was subjected to vigorous stirring for 8 h until complete homogenization and then sieved with a grain size of less than 0.45 mm being used unless stated otherwise. Finally, water was siphoned off, and the clay was dried in air at around 60 ± 1°C.

2.3. Characterization of adsorbent

The chemical composition was investigated using an XRF spectrometer (Axios, PANalytical, Holland). The samples were used in briquettes form containing 10 g of DE clay and pressed with 2.5 g of binder. Surface area was determined by adsorption-desorption of N_2 at 77 K with the Quantachrome Autosorb AS1C equipment.

The mineralogy of the raw clay and the adsorbent after fluoride sorption was examined using XRD (X'Pert PRO, PANalytical, Holland) with a Cu Kα radiation of 1.5406 Å at a scanning speed of 0.5° s^{-1}. The FTIR spectra were recorded on a Thermo Fisher Scientific 380 infrared spectrometer (Nicolet). The IR spectra were scanned between 500 and 4000 cm^{-1}, with a resolution of 4 cm^{-1}. The commercial software, OMNIC (Nicolet Instruments), was used for data acquisition and spectral analysis.

2.4. Industrial waste effluent

Real effluents from Tunisian aluminum fluoride industry were used in this study. AFMW were known by important fluctuations for the content of the element fluoride. So, five samples witch cover the range of variation of contents in this element were collected. Table 2 presents the compositions of the representative industrial effluent.

As can be seen from this table, these effluents to be treated were acidic with pH around 2, which have a high conductivity and are highly charged in fluoride. In contrast, silica, calcium, iron, and magnesium levels (scale-inducing ions) were low. High level of fluoride and low pHs confirm its toxicity and show that this kind of waters needs to be treated before it is discharged into the environment. For all fluoride-containing solutions, only polypropylene vessels were used for sample preparation and storage.

Table 2
Composition of a representative sample of AFMW

Parameters	Value
Conductivity at 25.0°C, mS/cm	195
Temperature, °C	25
pH	2
Silt density index (SDI), mL/g	0.01
Turbidity, NTU	90
Total suspended solids (TSS), mg/L	260
Total organic carbon (TOC), mg/L	36
Total Kjeldahl nitrogen (TKN), mg/L	2
Total phosphorus as P (TP), mg/L	4
Oil, fat and grease (FOG), mg/L	< 0.5
Cations	
Ca, mg/L	61
Mg, mg/L	32
Na, mg/L	1120
K, mg/L	1.5
Al, mg/L	381
Sr, mg/L	0.7
Ba, mg/L	0.7
Fe, mg/L	10
Mn, mg/L	< 0.05
Anions	
HCO_3, mg/L	< 1
NO_3, mg/L	< 1
Cl, mg/L	420
SO_4, mg/L	86
F, mg/L	1100
Other	
SiO_2, mg/L	1500
Free chlorine, mg/L	0.5

2.5. Instrumentation

The fluoride concentration in AFMW was determined using an ion selective electrode as per standard methods [55]. We used the Metrohm 781 pH/Ion meter equipped with an ion-selective electrode (Metrohm 6.0502.150) and Ag/AgCl reference electrode (Metrohm 6.0726.100).

The pH of the wastewater was measured using a Metrohm 780 pH Meter equipped by a HF resistant glass electrode (Metrohm 6.0421.100). The instrument was calibrated each time the analysis was done by using pH calibration buffers.

2.6. Batch experiments

Real wastewaters with initial fluoride concentrations ranging from 525 to 2003 mg/L were used. For every experiment, 200 mL of AFMW was taken into polypropylene bottle and known weight of adsorbent was added into it. The bottle was closed tightly and placed in a thermostated air bath shaker at 25 ± 1°C and a shaking speed of 350 rpm for 2 h to attain the equilibrium. The samples were collected every 10 min, filtered through a 0.45 µm membrane filter and the filtrate was analyzed for residual fluoride.

Next, kinetic batch experiments were performed at different initial fluoride concentrations namely 525, 1040 and 2003 mg/L. A desired volume of AFMW of desired concentration was transferred into the polypropylene bottles and a know mass of adsorbent was added to it. The suspension was stirred using horizontal orbital shaker at 350 rpm. Samples were withdrawn from the bottle frequently and analyzed for the concentration of fluoride by ion selective electrode.

The defluoridation capacity q was calculated according to the following mass balance equation:

$$q = (C_0 - C_e)\frac{V}{W} \tag{1}$$

where q (mg/g) is the amount of adsorbed fluoride, C_0 (mg/L) and C_e (mg/L) are the initial and equilibrium concentration of fluoride in the solution, respectively, W (g) is the dry weight of the adsorbent used and V (L) is the volume of fluoride solution.

3. Results and discussion

3.1. Characterization

3.1.1. XRF analysis

The chemical analysis of the clay is shown in Table 3, it can be noticed that the analyzed material is an aluminosilicate with high calcium content compared to the average of argillaceous minerals, due to the presence of calcic compounds in DE clay.

3.1.2. FTIR analysis

To get a better insight into the nature of the removal mechanism, FTIR spectra of the adsorbent before and after adsorption were recorded. The detected bands of the infrared spectra (Fig. 1a and 1b) are reported in Table 4a and 4b.

In the FTIR spectra of the clay before adsorption (Fig. 1a), a band recorded at 3636 cm^{-1} corresponded to O–H stretching vibrations for OH groups bonded to Al ions [56], a band recorded at 3375 cm^{-1} corresponded to the deformation bands of H–O–H. A band at 1646 cm^{-1} is the valence bands of O–H; the one at 1434 cm^{-1} was attributed to stretching vibration of C–O and is characteristic of presence of organic material [57]. The other peak at 1008 cm^{-1} was the valence bands of Si–O–Si [56]; that at 873 cm^{-1} of clay before adsorption from the deformation bands of Al–Mg–OH, and the band at 514 cm^{-1} from the deformation bands of Si–O–Al [58].

After adsorption of fluoride ions onto clay the peak at 795 cm^{-1} was due to the quartz [59], as shown in the XRD patterns. The peaks corresponding to hydroxyl and molecular water were affected. It was observed, for the adsorbent, that the intensity of peaks decreased which indicated that the surface hydroxyl groups on the adsorbent almost disappeared. Thus results showed the involvement of surface hydroxyl group in defluoridation of AFMW. Parallel obser-

Table 3
Chemical composition (in wt %) of the DE clay used in the experiment

SiO_2	30.7
Al_2O_3	7.5
CaO	26.3
Fe_2O_3	4.6
MgO	1.8
K_2O	0.6
SO_3	0.8
Na_2O	0.5
P_2O_5	0.1
TiO_2	0.4
ZnO	< 0.1
LOI*	26.5

*Loss on ignition at 975°C

Table 4
Attributions of bands observed by infrared spectroscopy for clay (a) before adsorption (b) after adsorption

Wave number (cm^{-1})	Assignment	Reference
(a)		
3636	υ1Al_2–OH υ4Al_2–OH υ_4Al_2–OH	[55]
3374	δ H–O–H	
1646	υ_{as} H–O–H	
1434	υ_{as} C–O	[57]
1008	υ_{as} Si–O–Si	[56]
873	δ Al–Mg–OH	
514	δ Si–O–Al	[58]
(b)		
2159	δ Ca–F	Present study
2034		
1023	υ_{as} Si–O–Si	[56]
795	υs Si–O–Si (quartz)	[59]
521	δ Si–O–Al	[58]

vations, i.e., complexation of calcium and aluminium with fluoride ions have been reported in literature related to the defluoridation of wastewater using calcium and aluminum salts [60–62]. However, none of these publications report the FTIR spectral evidence. Likewise, in the FTIR spectrum of DE clay after the adsorption (Fig. 1 b) of fluoride ions new intense peaks at 2034 and 2159 cm^{-1} were observed corresponding to the Ca–F bond. This observation suggests that the removal of fluoride ions by DE clay is by chemisorption.

3.1.3. XRD patterns

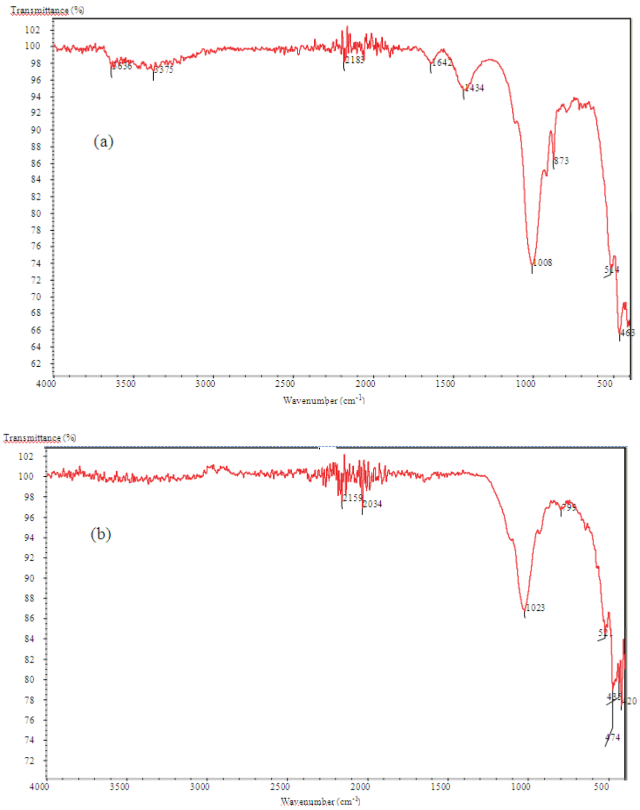

Fig. 1. FT-IR spectra of the samples: (a) DE clay before fluoride ion adsorption, (b) DE clay after fluoride ion adsorption.

The XRD patterns of the DE clay before and after treatment with fluoride ion were also recorded to confirm the mechanism of the adsorption process. Representative XRD patterns of DE clay before and after adsorption are depicted in Fig. 2a and 2b, respectively. As shown in Fig. 2a, the XRD pattern of this adsorbent shows some main peaks at diffraction angles of 2θ = 22.8, 26.5, 29.0, 30.8, 36.0, 39.6, 43.2, 47.5 and 48.6°. The peaks are strong and characterized by calcite, palygorskite and quartz. The other weak peaks are attributed to the presence of minor phases, such as phosphate, potassium and titanium. The XRD study of DE clay loaded with fluoride ions (Fig. 2b) showed significant changes when compared to that of DE before adsorption. This suggests that the uptake of fluoride ions by DE clay is by chemical adsorption which consequently alters the structure of the adsorbent. The reaction between fluoride ions and calcium to yield Ca–F bond is evident from the appearance of characteristic new peaks at 28.5 and 47° after adsorption. Hence, it is confirmed that, in the present study, fluoride ions are adsorbed by the adsorbent through chemisorption via the formation of Ca–F bond. On the other hand, there is no formation of Al–F although the DE clay used contains calcite and alumina. The high adsorption capacity of the adsorbent in thus attributed to the content of calcite in DE clay.

3.1.4. BET analysis

The specific surface area of the raw clay was found as 81 m^2/g. The low value of specific surface obtained for DE

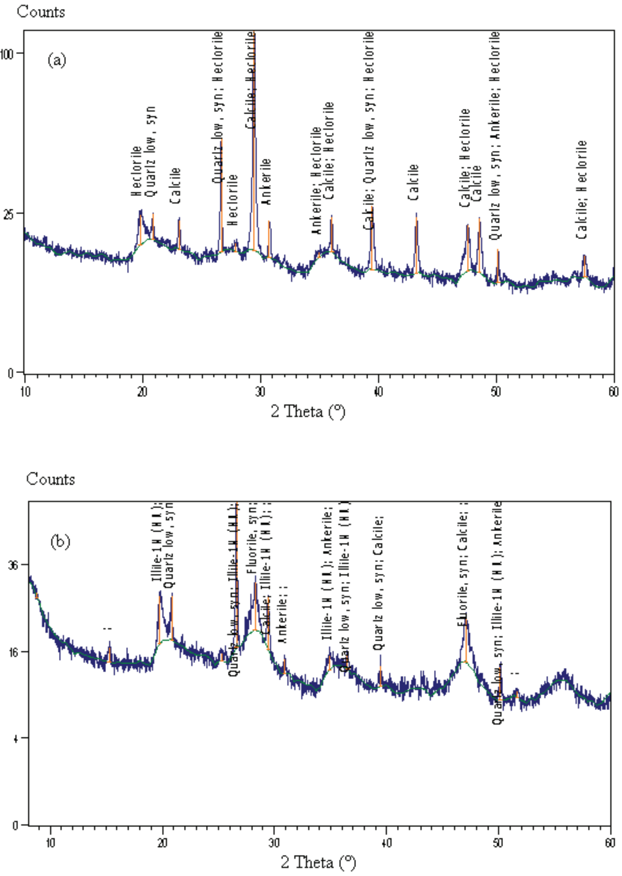

Fig. 2. XRD pattern of the samples: (a) DE clay before fluoride ion adsorption, (b) DE clay after fluoride ion adsorption.

clay compared to the montmorillonites whose specific surface varies from 600 to 700 m^2/g, is related to the presence of the impurities.

3.2. Effect of adsorbent amount

The effect of adsorbent dosage on the extent of fluoride removal was studied. The adsorbent amount was varied from 0.5 to 5 g/L for a contact time of 2 h. It can be seen that the DE sorbent exhibited excellent removal efficiency for fluoride. As shown in Fig. 3a, 2 g/L of DE clay can remove more than 97% of F$^-$ from 200 mL of 525 mg/L solution. Meanwhile, it was found that increasing the adsorbent dosage increased the percent removal until the percent removal approached to nearly 98%. For example, as the increase in DE clay amount from 0.5 to 2 g/L, the percent removal of F$^-$ increased rapidly from 73 to 97%. The concentration of surface hydroxyl groups is related to DE clay concentration through surface site density. With a further increase in DE clay dosage to 4 g/L, the percent removal increased to 98%. The results indicated that the DE clay can be used as efficient adsorbent for removal of fluoride from AFMW. For DE clay amounts above 4 g/L no significant increase in fluoride removal was observed (% removal of fluoride = 98% at an amount of DE clay 5 mg/L). Hence, 4 g/L is considered to be the optimum amount of the adsorbent for fluoride removal from AFMW. This parameter obtained in this study (4 g/L) is higher than the amount of 3 g/L reported by Thakre et al. [47] during studying of the defluoridation of drinking water by magnesium incorporated bentonite clay.

3.3. Influence of pH

It is well known that the pH of the aqueous solution plays an important role which controls the adsorption at the solid-water interface. Therefore, the effects of solution pH were studied in the range of 2–11. The effect of pH on the percentage removal of fluoride ion was examined at the initial fluoride concentration 2003 mg/L and temperature 25 ±1°C and the results are presented in Fig. 3b. It could be inferred that the fluoride removal decreases with increasing pH. The maximum fluoride removal was achieved at pH 2.0. Such types of adsorption behavior of fluoride had been reported for Algerian clay [44] but at pH of 4. This behavior might be due that at lower pH values, the surface of the clay will be surrounded by the hydrogen ions (positive charge) which enhance the fluoride adsorption through electrostatic attraction. However, at high pH, lower adsorption capacity of fluoride is due to the fact that the surface acquires negative charge in alkaline pH, and hence there is repulsion between the negatively charged surface and fluoride [63].

It was found that the pH changed during the treatment as shown in the Fig. 4. As it can be seen, for acid pHs, there is an increase of pH, while for alkaline pHs, the pH drops. There is noticeable neutralization phenomenon for acidic conditions resulting in pH increases.

3.4. Effect of initial fluoride concentration

The removal efficiency of fluoride at varying initial fluoride concentration in the range of 131–2003 mg L keeping other parameters constant is presented in Fig. 3c. Three trend stages of removal efficiency of fluoride variation were obtained: % removal increased quickly up from 131 to 256 mg/L, afterwards steep removal efficiency increase from 91 to 95% for 1040 mg/L, finally a pseudo plateau for high initial fluoride concentration reached. With the increase of the concentration of fluoride in solution, the availability of fluoride ions increases at the solid-solution interface, resulting in the increase of adsorption performance. Further the heterogeneous nature of the adsorbent with regard to the distribution of the binding sites predicts that the active sites are not equally effective. The sites which have a higher affinity for fluoride ion will have contributed more to adsorption.

3.5. Isotherm model

Equilibrium relationships between adsorbent and adsorbate are described by adsorption isotherms. The adsorption isotherm is important from both a theoretical and a practical point of view, isotherm data should be tested with different isotherm models to find a suitable model that can be used for the design of adsorption process. The two most commonly used isotherms, named Langmuir and Freundlich isotherms have been adopted [64]. The Langmuir theory is valid for monolayer adsorption onto a surface containing a finite number of identical sites and is one of

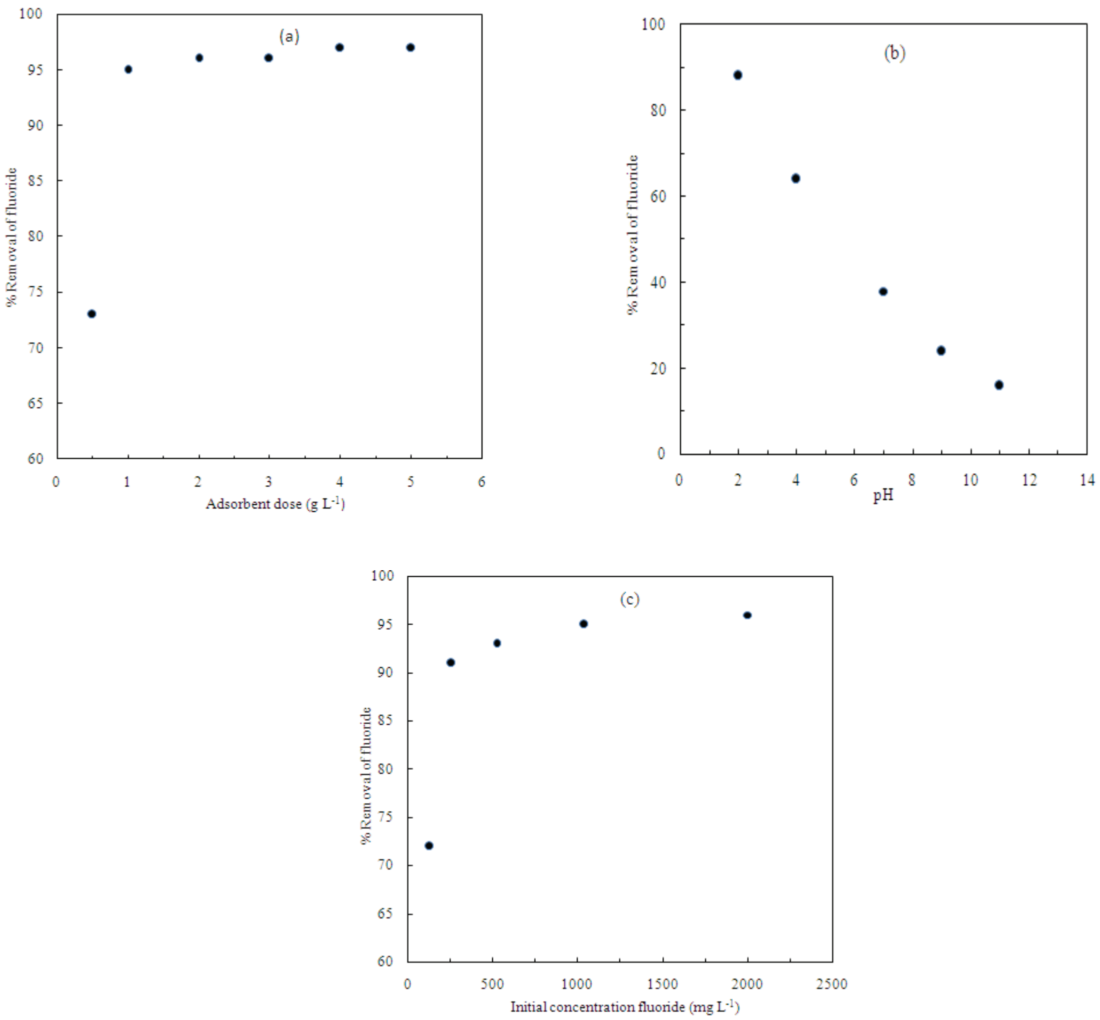

Fig. 3. Fluoride removal as function of: (a) adsorbent amount (volume of solution = 200 mL, equilibrium time = 120 min, temperature = 25.0 ± 1°C and shaken speed = 350 rpm), (b) pH (volume of solution = 200 mL, initial fluoride concentration = 2003 mg/L, equilibrium time = 120 min, temperature = 25.0 ± 1°C, clay amount = 4 g/L and shaken speed = 350 rpm), and (c) initial fluoride concentration (volume of solution = 200 mL, equilibrium time = 120 min, temperature = 25.0 ±1 °C, clay dose = 4 g/L and shaken speed = 350 rpm).

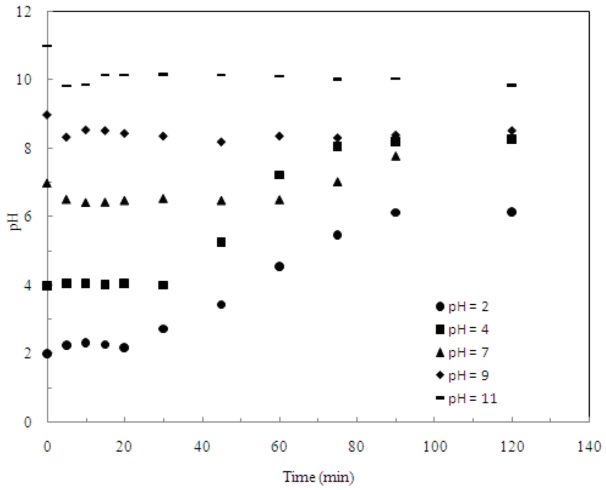

Fig. 4. Changes in pH with time during the treatment.

the most popular isotherm models due to its simplicity and its good agreement with experimental data. The Langmuir isotherm equation is expressed in the linear form as:

$$\frac{1}{q_e} = \frac{1}{Q_0} + \frac{1}{Q_0 K_L C_e} \qquad (2)$$

where q_e (mg/g) is the amount adsorbed at equilibrium; Q_0 (mg/g) is the maximum monolayer adsorption capacity; and K_L (L/mg) is the constant related to the free energy of adsorption. A linear plot is obtained for the sorbent when $1/q_e$ is plotted against $1/C_e$ which gives Q_0 and K_L values from the intercept and slope, respectively with the calculated results listed in Table 5.

The Freundlich isotherm model is an empirical equation and the model is valid for heterogeneous surfaces. It assumes that the adsorption process occurs on heterogeneous surfaces and the adsorption capacity is related to the concentration of fluoride at equilibrium.

The Freundlich model can be represented with the following linear equation:

$$\ln(q_e) = \ln(K_F) + \frac{1}{n}\ln(C_e) \tag{3}$$

where K_F (g mg^{-1}) is the empirical constant of Freundlich isotherm; the constant n is the empirical parameter related to the intensity of adsorption, which varies with the heterogeneity of the adsorbent. The Freundlich model parameters K_F and n are calculated from the slope and intercept of the plot (Fig. 5) of ln q_e vs. ln C_e, with the obtained results shown in Table 5.

Table 5
Values of Freundlich and Langmuir isotherm parameters of clay

Langmuir isotherm model			Freundlich isotherm model		
Q_0 (mg g^{-1})	K_L (L mg^{-1})	R^2	1/n	K_F (mg g^{-1})	R^2
334	0.0072	0.976	0.79	3.88	0.984

According to this table, it is found that the adsorption of fluoride on the DE clay was fit well with the Langmuir and Freundlich equation under the concentration range studied indicating possibility simultaneous validity of multiple isotherms. The magnitudes of 1/n lying between 0 and 1 and the n value lies in the range of 1–10 suggested that the adsorption of fluoride onto DE clay was quite favorable. Similarly, other investigators have also reported R^2 that are both high and close when fitted to the two models [65,66]. The comparison of Freundlich constants of different adsorbents for fluoride adsorption is given in Table 6.

3.6. Adsorption kinetics

The kinetic experiments were carried out at different initial concentrations at dose of 4 g/L. This kinetic study showed that a contact time of 120 min was sufficient to achieve equilibrium of fluoride. It was observed that the uptake of fluoride increase with time. However, the adsorption of fluoride was rapid in the first 30 min after which the rate slowed down as the equilibrium approached.

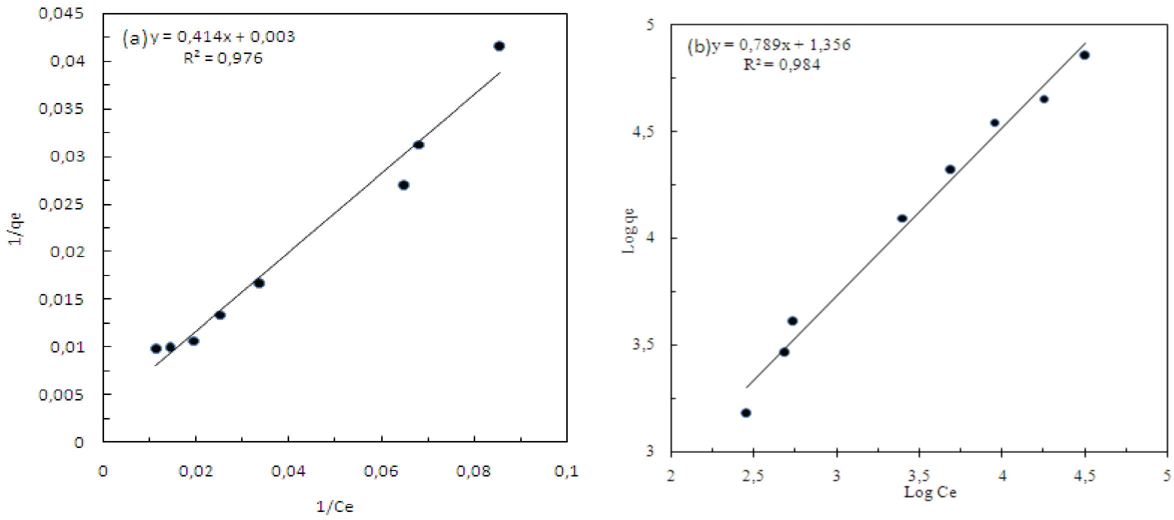

Fig. 5. Isotherm modeling for fluoride adsorption on clay (a) Langmuir isotherm; (b) Freundlich isotherm (clay amount 4 g L^{-1}, equilibrium contact time 120 min, initial pH 2 ± 0.1, temperature 25 ± 1 °C, shaking speed 350 rpm, and initial fluoride concentration = 131–2003 mg/L).

Table 6
The comparison of the Freundlich capacity constants for fluoride adsorption clays reported in the literature

Type of adsorbent used	K_F (mg/g)	n	Reference
Montmorillonite	0.26	1.77	[67]
Chemically modified bentonite clay	0.56	1.53	[46]
Granular acid-treated bentonite	0.094	2.082	[68]
Bentonite-based	0.135	2.978	[69]
Pyrophyllite clay particle size 0.42-0.85 mm	0.174	0.250	[70]
Pyrophyllite clay particle size 0.25-0.42 mm	0.213	0.224	[70]
Pyrophyllite clay particle size 0.15-0.25 mm	0.204	0.246	[70]
Pyrophyllite clay particle size < 0.15 mm	0.247	0.244	[70]
Tunisian clay	3.88	1.26	Present study

A pseudo-first-order model, and a pseudo-second-order model [71] were used to describe the adsorption kinetics of fluoride on DE clay. The mathematic equations representing the models are given as

Pseudo-first-order equation,

$$q_t - q_e\left(1 - \mathrm{e}^{\mathrm{k}_1 t}\right) \tag{4}$$

Pseudo-second-order equation,

$$q_t - \frac{q_e^2 k_2 t}{1 + q_e k_2 t} \tag{5}$$

In Eqs. (4) and (5), q_t (mg/g) is the adsorption amount at a given time t (min), and q_e (mg/g) is the adsorption equilibrium capacity at the final experimental time. In the equations, k_1 (min^{-1}), and k_2 (g/mg min) represent the adsorption rate constants for pseudo-first-order and pseudo-second-order adsorption, respectively. The linear forms of the pseudo-first and pseudo-second order equations are

$$\log(q_e - q_t) = \log q_e + \mathrm{k}_1 t \tag{6}$$

$$\frac{1}{q_t} = \frac{1}{q_e} + \frac{1}{q_e^2 k_2}\frac{1}{t} \tag{7}$$

By plotting log ($q_e - q_t$) versus time in Eq. (5) a straight line was obtained, from which the pseudo-first-order rate constant k_1 was obtained from the slope of the plot. According to Eq. (7) a plot of $1/q_t$ versus $1/t$ (Fig. 6) also generates a straight line and the values of q_e and k_2 can be calculated from the slope and intercept of this line. Fitting results of kinetics data by two models were shown in Table 7. As indicated in table, the R^2 values of pseudo-second-order model (> 0.98) were larger than that of pseudo-first-order model (≤ 0.972).

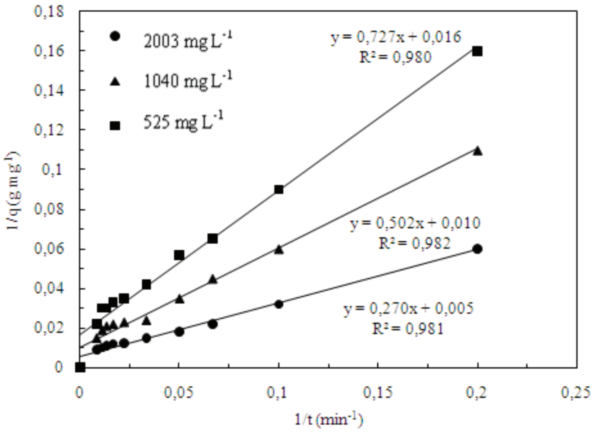

Fig. 6. Pseudo-second order kinetic for fluoride adsorption by DE clay.

As a result, we can say that the pseudo-second-order kinetic model suggested a better correlation for the adsorption of fluoride on the clay than the pseudo-first-order model. For most of the initial concentrations tested the pseudo-second-order rate constant k_2 was low, indicating that the rate of the fluoride adsorption process is fast. It was evident that the rate constant decreased with the initial feed concentrations. This can be attributed to the increased number of fluoride ions available for adsorption. Similar results have been obtained by Ma et al. [68] for the adsorption of fluoride onto acid-treated bentonite and by Fan et al. [72] onto low-cost materials.

In case of surface adsorption, a variation of adsorption rate should be proportional to the first power of concentration. The intra-particle diffusion model given by Weber and Morris is also commonly used to characterize the sorption data. In order to test the contribution of intra-particle diffusion on the adsorption process, the rate constant for intra-particle diffusion was obtained by using following equation.

$$q_t = k_p t^{1/2} \tag{8}$$

where k_p (mg/g min$^{1/2}$) is the intra-particle diffusion rate constant.

Fig. 7 shows the plot of kinetics data of fluoride removal by DE clay from AFMW solution as per Eq. (8). A linear correlation represents the control of sorption by intra particle diffusion and solute ions presumably diffuse within the pores and capillaries of the media and available sites for adsorption. The values of k_p calculated from the slope of the linear portions of the curves, are found as 1.4, 5.9 and 4.0 mg/g min$^{1/2}$ for initial concentration of 525, 1040 and 2003 mg/L of fluoride respectively (Table 7). The k_p values thus, increases initially with increasing fluoride concentrations (525 and 1040 mg/L), but decreases at 2003 mg/L. This shows that the adsorption is governed by intra-particle pore diffusion controlled with increasing concentration. The plot of the intra-particle pore diffusion present two plateaus it means that the kinetics adsorption of fluoride removal by DE clay is complex.

Table 7
Kinetics parameters of pseudo-first order, pseudo second order and intra particle pore diffusion parameters for clay at 25 ± 1 °C

C_0	Pseudo-first order		Pseudo-second order			Intra-particle diffusion constant	
(mg L^{-1})	k_1 (min^{-1})	R^2	10^{-2} k$_2$ (g/mg min^1)	q_e (mg/g)	R^2	K_p (mg/g min$^{1/2}$)	R^2
525	0.021	0.961	0.035	62.5	0.980	1.400	0.809
1040	0.018	0.954	0.019	100.0	0.982	4.986	0.905
2003	0.034	0.972	0.009	200.0	0.981	3.980	0.677

4. Conclusion

The results of this study demonstrate that the adsorption process was very efficient to reduce the concentration of fluoride anions in industrial wastewater of aluminum fluoride manufacturing in order to meet environmental regulation for wastewater discharge in terms of residual fluoride concentration. The adsorption process offers satisfactory results in terms of fluoride removals. The structure and the grade of calcite are the factor that contributes to the high adsorption capacity of fluoride. The results of the kinetic studies show that the equilibrium adsorption is practically achieved within 2 h. Also the observed kinetics behavior for the DE clay is better explained by the pseudo-second-order kinetic model. Both external and intra-particle diffusion contribute to the rate of removal of fluoride on the DE clay. However, the intra-particle diffusion is slow at low concentrations. The experimental sorption isotherm results indicate that both the Langmuir and Freundlich adsorption isotherm represent well the fluoride adsorption on the adsorbent. The foregoing results and discussions indicated that the adsorption occurs through chemisorptions, i.e., via the formation of Ca–F bond. The adsorption can only reduce the fluoride concentration to 10 mg/L against 5 mg/L maximum value according the Tunisian standard. Consequently, another defluoridation process must be performed.

These experimental data obtained in this study, demonstrated that the DE clay appears to be a promising, environmental friendly material, and cost-effective alternative sorbent for removing fluoride from industrial wastewater. However discharge of a large quantity of residual solid and difficulty in regeneration of clay should be considered.

Acknowledgements

Thanks are extended to Dr Nabil FETTEH, Head of Department of Mineralogy and Rock Mechanics at Company Phosphate Gafsa for facilitating the analysis of samples using X-ray diffractometer (XRD).

References

[1] M. Bhardwaj, S. Aggarwal, Evaluation of biochemical interaction and correlation between high fluoride ingestion and protein metabolism, Biomed. Prev. Nutr., 3(2) (2013) 129–137.

[2] H.L. Liu, Q. Zeng, Y.S. Cui, L.Y. Yu, L. Zhao, C.C. Hou, S. Zhang, L. Zhang, G. Fu, Y.M. Liu, C.Y. Jiang, X.M. Chen, A.G. Wang, The effects and underlying mechanism of excessive iodide on excessive fluoride-induced thyroid cytotoxicity, Environ. Toxicol. Pharmacol., 38(1) (2014) 332–340.

[3] EPA, Federal Water Pollution Control Act (Clean Water Act), Semiconductor Best Practicable Control Technology Currently Available (BPT) Effluent Limitations, Available June 23, 2015 from: http://www.epa. gov/dfe/pubs/pwb/tech_rep/fedregs/regsectb.htm.

[4] Tunisian standard NT.106.002 relative to wastewaters (Environmental protection), Off. J. Tunisian Repub., 59 (1989) 1332–1338.

[5] M. Yang, T. Hashimito, N. Hoshi, H. Myoga, Fluoride removal in a fixed bed packed with granular calcite, Water Res., 33 (1999) 3395–3402.

[6] F. Shen, X. Chen, P. Gao, G. Chen, Electrochemical removal of fluoride ions from industrial wastewater, Chem. Eng. Sci., 58 (2003) 987–993.

[7] JORF, Decree of September 26 1985 regarding surface finishing units (in French). Available 23 June 2015 from: http://www.legifrance.gouv.fr/affichTexte.do.

[8] B. Grzmil, J. Wronkowski, Removal of phosphates and fluorides from industrial wastewater, Desalination, 189 (2006) 261–268.

[9] A. Toyoda, T. Taira, A new method for treating fluorine wastewater to reduce sludge and running costs, IEEE T. Semiconduct. M., 13(3) (2000) 305–309.

[10] V.K. Gupta, R. Jain, A. Mittal, T.A. Saleh, A. Nayak, S. Agarwal, S. Sikarwar, Photo-catalytic degradation of toxic dye amaranth on TiO_2/UV in aqueous suspensions, Mater. Sci. Eng. C., 32(1) (2012) 12–17.

[11] T.A. Saleh, V.K. Gupta, Column with CNT/magnesium oxide composite for lead(II) removal from water, Environ. Sci. Pollut. Res., 19(4) (2012) 1224–1228.

[12] V.K. Gupta, S.K. Srivastava, D. Mohan, S. Sharma, Design parameters for fixed bed reactors of activated carbon developed from fertilizer waste for the removal of some heavy metal ions, Waste Manage., 17(8) (1998) 517–522.

[13] A. Mittal, J. Mittal, A. Malviya D. Kaur, V.K. Gupta, Decoloration treatment of a hazardous triarylmethane dye, Light Green SF (Yellowish) by waste material adsorbents, J. Colloid Interf. Sci., 342(2–15) (2010) 518–527.

[14] A. Mittal, D. Kaur, A. Malviya, J. Mittal, V.K. Gupta, Adsorption studies on the removal of coloring agent phenol red from wastewater using waste materials as adsorbents, J. Colloid Interf. Sci., 337(2) (2009) 345–354.

[15] A. Mittal, A. Malviya, V.K. Gupta, Adsorptive removal of hazardous anionic dye "Congo red" from wastewater using waste materials and recovery by desorption, J. Colloid Interf. Sci., 340(1) (2009) 16–26.

[16] A. Mittal, J. Mittal, A. Malviya, V.K. Gupta, Removal and recovery of Chrysoidine Y from aqueous solutions by waste materials, J. Colloid Interf. Sci., 344(2) (2010) 497–507.

[17] V.K. Gupta, R. Jain, A. Nayak, S. Agarwal, M. Shrivastava, Removal of the hazardous dye—Tartrazine by photodegradation on titanium dioxide surface, Mater. Sci. Eng. C., 31(5) (2011) 1062–1067.

[18] V.K. Gupta, R. Jain, A. Nayak, S. Agarwal, M. Shrivastava, Cadmium removal and recovery from aqueous solutions by novel adsorbents prepared from orange peel and Fe_2O_3 nanoparticles, Chem. Eng. J., 180 (2012) 81–90.

[19] T.A. Saleh, V.K. Gupta, Photo-catalyzed degradation of hazardous dye methyl orange by use of a composite catalyst consisting of multi-walled carbon nanotubes and titanium dioxide, J. Colloid Interf. Sci., 371(1) (2012) 101–106.

[20] H. Khani, M.K. Rofouei, P. Arab, V.K. Gupta, Z. Vafaei, Multi-walled carbon nanotubes-ionic liquid-carbon paste electrode as a super selectivity sensor: Application to potentiometric monitoring of mercury ion(II), J. Hazard. Mater., 183(1–3), (2010) 402–409.

[21] S. Karthikeyan, V.K. Gupta, R. Boopathy, A. Titus, G. Sekaran, A new approach for the degradation of high concentration of aromatic amine by heterocatalytic Fenton oxidation: Kinetic and spectroscopic studies, J. Mol. Liquids, 173 (2012) 153–163.

[22] A.K. Jain, V.K. Gupta, A. Bhatnagar, A comparative study of adsorbents prepared from industrial wastes for removal of dyes, Separ. Sci. Technol., 38(2) (2003) 463–481.

[23] V.K. Gupta, A. Nayak, S. Agarwal, Bioadsorbents for remediation of heavy metals: Current status and their future prospects, Environ. Eng. Res., 20(1) (2015) 001–018.

[24] T.A. Saleh, V.K. Gupta, Processing methods, characteristics and adsorption behavior of tire derived carbons: A review, Adv. Colloid Interface Sci., 21 (2014) 92–100.

[25] V.K. Gupta, R. Kumar, A. Nayak T.A. Saleh, M.A. Barakat, Adsorptive removal of dyes from aqueous solution onto carbon nanotubes: A review, Adv. Colloid Interface Sci., 193(194), (2013) 24–34.

[26] R. Saravanan, E. Sacari, F. Gracia, M.M. Khan, E. Mosquera, V.K. Gupta, Conducting PANI stimulated ZnO system for visible light photocatalytic degradation of coloured dyes, J. Mol. Liq., 221 (2016) 1029–1033.

[27] M. Devaraj, R. Saravanan, R.K. Deivasigamani, V.K. Gupta, F. Gracia, S. Jayadevan, Fabrication of novel shape Cu and Cu/Cu_2O nanoparticles modified electrode for the determination of dopamine and paracetamol, J. Mol. Liq., 221 (2016) 930–941.

[28] S. Rajendran, M.M. Khan, F. Gracia, J. Qin, V.K. Gupta, S. Arumainathan, Ce^{3+}-ion-induced visible-light photocatalytic degradation and electrochemical activity of ZnO/CeO_2 nanocomposite, Scientific Reports, 6 (2016) 31641.

[29] R. Saravanan, V.K. Gupta, E. Mosquera, F. Gracia, V. Narayanan, A. Stephen, Visible light induced degradation of methyl orange using β-Ag0.333V2O5 nanorod catalysts by facile thermal decomposition method, J. Saudi Chem. Soc., 19(5) (2015) 521–527.

[30] R. Saravanan, F. Gracia, M.M. Khan, V. Poornima, V.K. Gupta, V. Narayanan, A. Stephen, ZnO/CdO nanocomposites for textile effluent degradation and electrochemical detection, Mol. Liq., 209 (2015) 374–380.

[31] R. Saravanan, M.M. Khan, V.K. Gupta, E. Mosquera, F. Gracia, V. Narayanan, A. Stephen, ZnO/Ag/Mn_2O_3 nanocomposite for visible light-induced industrial textile effluent degradation, uric acid and ascorbic acid sensing and antimicrobial activity, RSC Advances, 5 (2015) 34645–34651.

[32] A. Bhatnagar, E. Kumar, M. Sillanpää, Fluoride removal from water by adsorption - A review, Chem. Eng. J., 171(3) (2011) 811–840.

[33] R. Leyva-Ramos, N.A. Medellin-Castillo, A. Jacobo-Azuara, J. Mendoza-Barron, L.E. Landin-Rodriguez, J.M. Martinez-Rosales, A. Aragon-Piña, Fluoride removal from water solution by adsorption on activated alumina prepared from pseudo-boehmite, J. Environ. Eng. Manage., 18(5) (2008) 301–309.

[34] J.Q. Ma, Y. Shen, C.S. Shen, Y.Z. Wen, W.P. Liu, Al-doping chitosan-Fe(III) hydrogel for the removal of fluoride from aqueous solutions, Chem. Eng. J., 248 (2014) 98–106.

[35] W. Xiang, G.K. Zhang, Y.L. Zhang, D.D. Tang, J.T. Wang, Synthesis and characterization of cotton-like Ca-Al-La composite as an adsorbent for fluoride removal, Chem. Eng. J., 250 (2014) 423–430.

[36] J. Wang, X.Y. Lin, X.G. Luo, Y.F. Long, A sorbent of carboxymethyl cellulose loaded with zirconium for the removal of fluoride from aqueous solution, Chem. Eng. J., 252 (2014) 415–422.

[37] D. Dayananda, V.R. Sarva, S.V. Prasad, J. Arunachalam, N.N. Ghosh, Preparation of CaO loaded mesoporous Al_2O_3: Efficient adsorbent for fluoride removal from water, Chem. Eng. J., 248 (2014) 430–439.

[38] T. Nur, P. Loganathan, T.C. Nguyen, S. Vigneswaran, G. Singh, J. Kandasamy, Batch and column adsorption and desorption of fluoride using hydrous ferric oxide: Solution chemistry and modeling, Chem. Eng. J., 247 (2014) 93–102.

[39] M. Mohapatra, S. Anand, B.K. Mishra, D.E. Giles, P. Singh, Review of fluoride removal from drinking water, J. Environ. Manage., 91(1) (2009) 67–77.

[40] A.K. Chaturvedi, K.C. Pathak, V.N. Singh, Fluoride removal from water by adsorption on china clay, Appl. Clay Sci., 3(4) (1988) 337–346.

[41] G. Karthikeyan, A. Pius, G. Alagumuthu, Fluoride adsorption studies of montmorillonite clay, Indian J. Chem. Technol., 12(3) (2005) 263–272.

[42] L. Lv, Defluoridation of drinking water by calcined MgAl-CO_3 layered double hydroxides, Desalination, 208(1–3) (2007) 125–133.

[43] A. Ramdani, S. Taleb, A. Benghalem, N. Ghaffour, Removal of excess fluoride ions from Saharan brackish water by adsorption on natural materials, Desalination, 250(1) (2010) 408–413.

[44] P.K. Gogoi, R. Baruah, Fluoride removal from water by adsorption on acid activated kaolinite clay, Indian J. Chem. Technol., 15(5) (2008) 500–503.

[45] S.P. Kamble, P. Dixit, S.S. Rayalu, N.K. Labhsetwar, Defluoridation of drinking water using chemically modified bentonite clay, Desalination, 249(2) (2009) 687–693.

[46] D. Thakre, S. Rayalu, R. Kawade, S. Meshram, J. Subrt, N. Labhsetwar, Magnesium incorporated bentonite clay for defluoridation of drinking water, J. Hazard. Mater., 180(1–3) (2010) 122–130.

[47] S. Gammoudi, N. Frini-Srasra, E. Srasra, Preparation, characterization of organosmectites and fluoride ion removal, Int. J. Miner. Process., 125 (2013) 10–17.

[48] I. Ghorbel-Abid, K. Galai, M. Trabelsi-Ayadi, Retention of chromium (III) and cadmium (II) from aqueous solution by illitic clay as a low-cost adsorbent, Desalination, 256(1–3) (2010) 190–195.

[49] M. Eloussaief, M. Benzina, Efficiency of natural and acid-activated clays in the removal of Pb(II) from aqueous solutions, J. Hazard. Mater., 178(1–3) (2010) 753–757.

[50] M. Eloussaief, N. Kallel, A. Yaacoubi, M. Benzina, Mineralogical identification, spectroscopic characterization, and potential environmental use of natural clay materials on chromate removal from aqueous solutions, Chem. Eng. J., 168(3) (2011) 1024–1031.

[51] M. Mhamdi, H. Galai, N. Mnasri, E. Elaloui, M. Trabelsi-Ayadi, Adsorption of lead onto smectite from aqueous solution, Environ. Sci. Pollut. R., 20(3) (2013) 1686–1697.

[52] M. Mhamdi, E. Elaloui, M. Trabelsi-Ayadi, Adsorption of zinc by a Tunisian Smectite through a filtration membrane, Ind. Crop. Prod., 47 (2013) 204–211.

[53] A. Amari, M. Chlendi, A. Gannouni, A. Bellagi, Optimised activation of bentonite for toluene adsorption, Appl. Clay Sci., 47(3–4) (2010) 457–461.

[54] APHA, Standard Methods for the Examination of Water and Wastewater. 19th Ed., American Public Health Association, Washington, DC (1998).

[55] J. Madéjova, FTIR techniques in clay mineral studies, Vib. Spectrosc., 31(1) (2003) 1–10.

[56] P. Salerno, S. Mendioroz, Preparation of Al-pillared montmorillonite from concentrated dispersions, Appl. Clay Sci., 22(3) (2002) 115–123.

[57] V.C. Farmer, The Infrared Spectra of Minerals, The Mineralogical Society, London. (1974) 331–364.

[58] M. Criado, A. Fernandez-Jimenez, A. Palomo, Alkali activation of fly ash: Effect of the SiO_2/Na_2O ratio Part I: FTIR study, Micropor. Mesopor. Mat., 106(1–3) (2007) 180–191.

[59] A. Ezzeddine, A. Bedoui, A. Hannachi, N. Bensalah, Removal of fluoride from aluminum fluoride manufacturing wastewater by precipitation and adsorption processes, Desalin. Water Treat., 54(8) (2015) 2280–2292.

[60] S. Saha, Treatment of aqueous effluent for fluoride removal, Water Res., 27(8) (1993) 1347–1350.

[61] A.L. Valdivieso, J.L.R. Bahena, S. Song, R.H. Urbina, Temperature effect on the zeta potential and fluoride adsorption at the α-Al_2O_3/aqueous solution interface, J. Colloid Interf. Sci., 298(1) (2006) 1–5.

[62] C.S. Sundaram, N. Viswanathan, S. Meenakshi, Uptake of fluoride by nano-hydroxyapatite/chitosan, a bioinorganic composite, Biores. Technol., 99(17) (2008) 8226–8230.

[63] W.G. Kim, M.N. Kim, S.M. Lee, J.K. Yang, Removal of Cu(II) with hydroxyapatite (animal bone) as an inorganic ion exchanger, Desalin. Water Treat., 4(1–3) (2009) 269–273.

[64] S. Gao, J. Cui, Z.G. Wei, Study on the fluoride adsorption of various apatite materials in aqueous solution, J. Fluorine Chem., 130(11) (2009) 1035–1041.

[65] B. Kemer, D. Ozdes, A. Gundogdu, V.N. Bulut, C. Duran, M. Soylak, Removal of fluoride ions from aqueous solution by waste mud, J. Hazard. Mater., 168(2–3) (2009) 888–894.

[66] A. Tor, Removal of fluoride from an aqueous solution by using montmorillonite, Desalination, 201(1–3) (2006) 267–276.

[67] Y.X. Ma, F.M. Shi, X.L. Zheng, J. Ma, C.J. Gao, Removal of fluoride from aqueous solution using granular acid-treated bentonite (GHB): Batch and column studies, J. Hazard. Mater., 185(2–3) (2011) 1073–1080.

[68] J.F. Ma, J. Qi, C. Yao, B.Y. Cui, T.L. Zhang, D.L. Li, A novel bentonite-based adsorbent for anionic pollutant removal from water, Chem. Eng. J., 200 (2012) 97–103.

[69] J.H. Kim, C.G. Lee, J.A. Park, J.K. Kang, N.C. Choi, S.B. Kim, Use of pyrophyllite clay for fluoride removal from aqueous solution, Desalin. Water Treat., 51(16–18) (2013) 3408–3416.

[70] X.M. Dou, Y.S. Zhang, H.J. Wang, T.J. Wang, Y.L. Wang, Performance of granular zirconium-iron oxide in the removal of fluoride from drinking water, Water Res., 45(12) (2011) 3571–3578.

[71] X. Fan, D.J. Parker, M.D. Smith, Adsorption kinetics of fluoride on low cost materials, Water Res., 37(20) (2003) 4929–4937.